Near Infrared Absorption of Pure Carbon Dioxide up to 3100 bar and 500 K
II. Wavenumber Range 5600 cm^{-1} to 7400 cm^{-1}

M. Buback, J. Schweer, and H. Tups
Institut für Physikalische Chemie der Universität Göttingen

Z. Naturforsch. **41 a**, 512–518 (1986); received December 7, 1985

Near infrared absorption of pure CO_2 in the $3\nu_1 + \nu_3$, $2\nu_1 + 2\nu_2^0 + \nu_3$, $\nu_1 + 4\nu_2^0 + \nu_3$, $6\nu_2^0 + \nu_3$ Fermi tetrad region around 6300 cm^{-1} and in the $3\nu_3$ second overtone region around 6970 cm^{-1} was measured at temperatures between 298 K and 500 K to a maximum pressure of 3100 bar. The $3\nu_3$ bandshape, at moderate compression up to 0.1 $g \cdot cm^{-3}$, is adequately represented by summing over individual rotation-vibration lines with half-widths proportional to the density. Band maximum positions and vibrational intensities between gaseous and liquid-like states are reported and discussed. Promising applications of high-pressure high-temperature near infrared spectroscopy to the quantitative analysis of CO_2 are illustrated for the 3200 cm^{-1} to 7400 cm^{-1} region. The technique can be used for CO_2 concentrations or at optical path lengths differing by several orders of magnitude.

1. Introduction

Near infrared (NIR) spectroscopy enables direct quantitative studies on fluids up to high pressures and temperatures [1]. Toward higher overtone and combination modes the vibrational intensities strongly decrease. NIR intensities are by about one and up to several orders of magnitude below corresponding fundamental mode intensities. Via NIR spectroscopy, chemical reactions and equilibria, even in highly concentrated dense systems, can be measured within a wide range of optical pathlengths, typically from about one up to several hundred millimeters. The potential of the method in kinetic investigations, e.g. in the process control of fluid phase reactions, is largely enhanced by the availability of NIR Fourier transform equipment scanning the whole wavenumber range between 3000 cm^{-1} and 12000 cm^{-1} in less than one second. In addition to these applications in quantitative analysis, high-pressure high-temperature NIR spectroscopy provides information about structure and dynamics in fluids.

The number of papers dealing with fluid state NIR spectroscopy, even of simple molecules, is surprisingly low. NIR absorption of pure CO_2 between 3200 cm^{-1} and 5600 cm^{-1} is investigated up to 3100 bar and 500 K in Part I of this series [2]. The aim of the present paper is to study, within the same pressure and temperature range, the density and temperature dependence of band position, vibrational intensity, and bandshape in the 5600 cm^{-1} to 7400 cm^{-1} wavenumber region of CO_2 with special emphasis on the stretching second overtone $3\nu_3$ which is remarkable in that no Fermi resonance coupling exists to any other mode.

Reprint requests to Prof. Dr. M. Buback, Institut für Physikalische Chemie der Universität Göttingen, Tammannstraße 6, D-3400 Göttingen.

2. Experimental

Information about the experimental set-up and about the optical equipment is provided in Part I [2]. Reported maximum wavenumbers (band positions) are accurate within ± 1 cm^{-1} due to the occurrence of relatively broad bands. Vibrational intensities (integrated molar absorptivities) are determined from the equation

$$B = \int \varepsilon(\bar{\nu}) \cdot d\bar{\nu}, \quad (1)$$

where the molar absorptivity $\varepsilon(\bar{\nu})$ is calculated according to

$$\varepsilon(\bar{\nu}) = A(\bar{\nu})/(c\,l). \quad (2)$$

$A(\bar{\nu})$ is the decadic absorbance, c the actual concentration (or density), and l the optical path length at experimental pressure and temperature. Due to several sources of error, the uncertainty in B is

0340-4811 / 86 / 0300-0512 $ 01.30/0. – Please order a reprint rather than making your own copy.

± 6%. Only at the lowest experimental densities it can be as large as ± 10%.

3. Results

NIR absorption of CO_2 between 5600 cm^{-1} and 7400 cm^{-1} consists of two band systems centered around 6300 cm^{-1} and 6970 cm^{-1}, respectively. In Fig. 1, absorbance spectra in the 6300 cm^{-1} region, which are assigned to the $3\nu_1 + \nu_3$, $2\nu_1 + 2\nu_2^0 + \nu_3$, $\nu_1 + 4\nu_2^0 + \nu_3$, $6\nu_2^0 + \nu_3$ Fermi tetrad, are shown for 400 K and several densities varying from bottom to top in steps of 0.1 g · cm^{-3} between 0.1 g · cm^{-3} (66 bar) and 1.2 g · cm^{-3} (3100 bar). The bands are shifted in the baseline to avoid intersection. With increasing density, the contour of each of the main bands gradually transforms from a P- and R-branch envelope into a single fairly symmetric component. At the highest densities, additional weak bands or shoulders are clearly observed. The components at 6190 cm^{-1} and 6530 cm^{-1} are assigned to hot-band transitions [3].

Absorbance spectra of the stretching second overtone $3\nu_3$ around 6950 cm^{-1} are given in Fig. 2 for densities varying (from bottom to top) in steps of 0.1 g · cm^{-3} between 0.1 g · cm^{-3} (54 bar) and 1.2 g · cm^{-3} (2300 bar) at 350 K. With increasing density, the band contour with a pronounced R-branch at 6980 cm^{-1} transforms into an intense band with a low-frequency shoulder. Closer inspection of the 0.1 g · cm^{-3} spectrum (Fig. 2) in the wavenumber region around 6960 cm^{-1} indicates that this absorption is not exclusively due to the P-branch of a single $3\nu_3$ transition. A detailed band analysis is presented in the subsequent section together with a discussion of the density and temperature dependencies of the peak positions and vibrational intensities in the 5600 cm^{-1} to 7400 cm^{-1} NIR range.

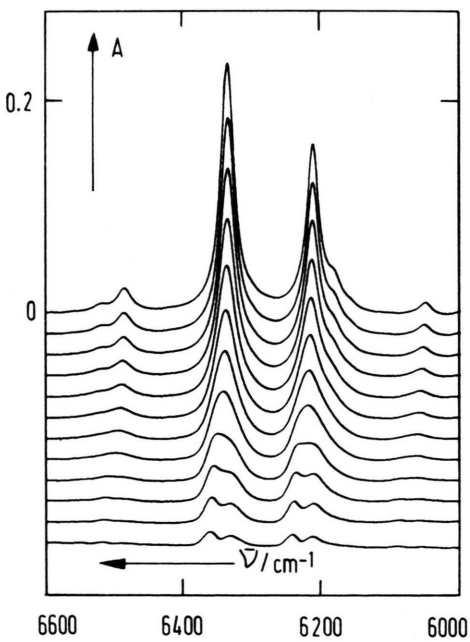

Fig. 1. Near infrared absorbance spectra of pure CO_2 at 400 K and densities varying – from bottom to top – in steps of 0.1 g · cm^{-3} between 0.1 g · cm^{-3} (66 bar) and 1.2 g · cm^{-3} (3100 bar).

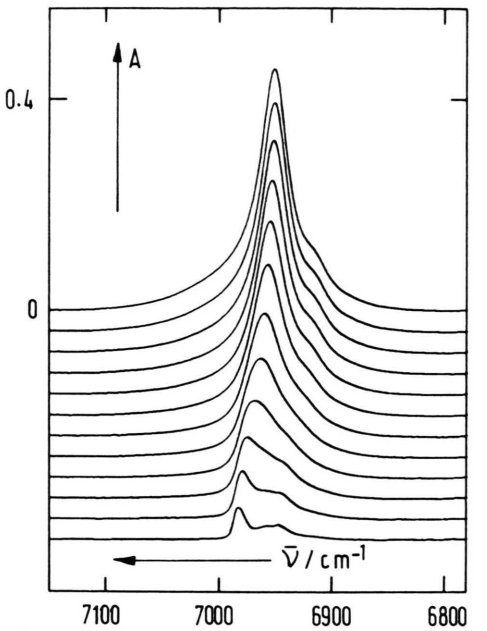

Fig. 2. Absorbance spectra of the stretching second overtone $3\nu_3$ of pure CO_2 at 350 K and densities varying – from bottom to top – in steps of 0.1 g · cm^{-3} between 0.1 g · cm^{-3} (54 bar) and 1.2 g · cm^{-3} (2300 bar).

4. Discussion

The interpretation of CO_2 near infrared spectra is complicated because of the ν_1, $2\nu_2^0$ Fermi resonance interaction through which most of the combination modes are coupled as has been demonstrated for the $\nu_1 + \nu_3$, $2\nu_2^0 + \nu_3$ Fermi diad and for the $2\nu_1 + \nu_3$, $\nu_1 + 2\nu_2^0 + \nu_3$, $4\nu_2^0 + \nu_3$ Fermi triad in Part I of this

series [2]. Within the 3200 cm^{-1} to 7400 cm^{-1} wavenumber range only the second overtone $3\nu_3$ around 6970 cm^{-1} is free from any Fermi coupling and thus should yield the density and temperature dependence of a pure stretching mode. Literature data on the high resolution gas spectrum, however, indicate that a hot-band $3\nu_3$ transition from the first excited level of the ν_2 bending fundamental may contribute to the absorption around 6950 cm^{-1} [4–6]. Thus bandshapes at moderate and high temperatures are not adequately represented by a single P- and R-type contour as has already been observed from the 0.1 g · cm^{-3} spectrum in Figure 2.

The temperature variation at constant density clearly shows the overlap of at least two P- and R-branch systems as is demonstrated in Fig. 3 with experimental CO_2 spectra at 0.2 g · cm^{-3} and temperatures varying from 298 K to 500 K. The room temperature spectrum essentially consists of the (00^03)-(00^00) Σ-Σ transition with an intense R-branch around 6980 cm^{-1} and a P-branch (shoulder) at about 6960 cm^{-1}. The 500 K spectrum, in addition, shows the R-branch of the (01^13)-(01^10) Π-Π hot-band transition with maximum values of R- and P-branches at 6950 cm^{-1} and around 6920 cm^{-1}, respectively. (The decrease of R-branch half-width toward higher temperature is due to a band-head behaviour which is known from gas phase literature data [4–6]).

Discussion of the $3\nu_3$ bandshape thus has to be based on parameters of (at least) these two transitions. A model developed by Bouanich et al. [7, 8] enables the reduced molar absorptivity band contour $\varepsilon_n(\bar{\nu}) = \varepsilon(\bar{\nu})/B$ at moderate compression to be represented by parameters of the low density gas spectrum (B is defined as in (1)). The band profile is generated by summing over the individual rotation-vibration lines with half-widths proportional to density. The line positions are the gas-phase literature data with a small correction for the actual density, which is assumed to be independent of the rotational quantum number m and thus is obtained from the density dependence of the experimental band maximum. A single adjustable parameter α modifies the individual line-profiles from purely Lorentzian ($\alpha = 0$) to almost Gaussian shape at $\alpha = 1$. The equations are given in Bouanich's papers [7, 8]. They are also included in a recent study on the NIR absorption of pure carbon monoxide where the experimental bandshape, almost up to the critical density, could be adequately represented by this procedure [9].

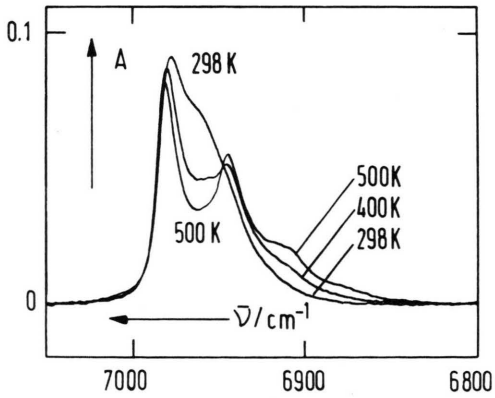

Fig. 3. Stretching second overtone $3\nu_3$ absorbance of pure CO_2 at 0.2 g · cm^{-3} and several temperatures.

The CO_2 band contour $\varepsilon_n(\bar{\nu})$ has to be described by a Boltzmann weighted sum of the ground state and hot-band $3\nu_3$ contours $\varepsilon_{n,l}(\bar{\nu})$ according to

$$\varepsilon_n(\bar{\nu}) = \frac{\sum_{l=0}^{1} (g_l \cdot \exp(-E_{\mathrm{vib}}/kT)) \cdot \varepsilon_{n,l}(\bar{\nu})}{\sum_{l=0}^{1} (g_l \cdot \exp(-E_{\mathrm{vib}}/kT))} . \quad (3)$$

The statistical weights are $g_l = 1$ for the quantum number $l = 0$ and $g_l = 2$ for $l = 1$ [10]. The Σ-Σ ground state transitions refer to $l = 0$ whereas the hot-band Π-Π transitions occur between vibrational levels with $l = 1$. E_{vib} is the lower state vibrational energy. $\varepsilon_{n,l}(\bar{\nu})$ is given in paper [9]. Line positions in the dilute gas are published for the ground state and hot-band transition of $3\nu_3$ [4–6]. Unfortunately, Lorentzian half-widths γ_0 at low density reference states are not available. Using published data on other gaseous CO_2 modes with identical symmetry [10–12], the reference state (298.15 K, 1.013 bar) values $\gamma_0(|m|)$ as a function of rotational quantum number m are estimated to be

$$\gamma_0(|m|)/\mathrm{cm}^{-1} = 0.120 - 0.001 \cdot |m| . \quad (4)$$

The half-width $\gamma(|m|)$ at the density ϱ is determined from $\gamma_0(|m|)$ at the reference density ϱ_0 according to

$$\gamma(|m|) = \gamma_0(|m|)\, \varrho/\varrho_0 . \quad (5)$$

Spectra calculated according to (3)–(5), at moderate compression, are in fair agreement with experimental data as is illustrated for 0.1 g · cm^{-3}

CO_2 density at 400 K in the upper part of Figure 4. Slight differences between the two band profiles only occur in the region of the weak shoulder around 6955 cm^{-1}. Toward higher density, the model works less satisfactory. At 0.2 $g \cdot cm^{-3}$ density and 500 K, corresponding to 145 bar, the model already overestimates the broadening of the P- and R-branches. The discrepancies are partly due to the lack of measured half-width data in the gaseous state. But even with perfectly known line positions and gaseous half-widths, and if only unpolar materials are studied, calculation of compressed state spectra from these data is certainly limited to densities below the critical one ($\varrho_c(CO_2) = 0.45\ g \cdot cm^{-3}$). An interesting feature of the method, however, relates to the ease by which, from a knowledge of the dilute gas spectrum, overlapping bands in moderately compressed gases are represented as a sum over individual bands and thus may be resolved without using empirical functions. The P- and R-type contour of the Σ-Σ and Π-Π (hot-band) $3\nu_3$ transition, which occur as a by-product in the calculations are shown in the lower part of Figure 4.

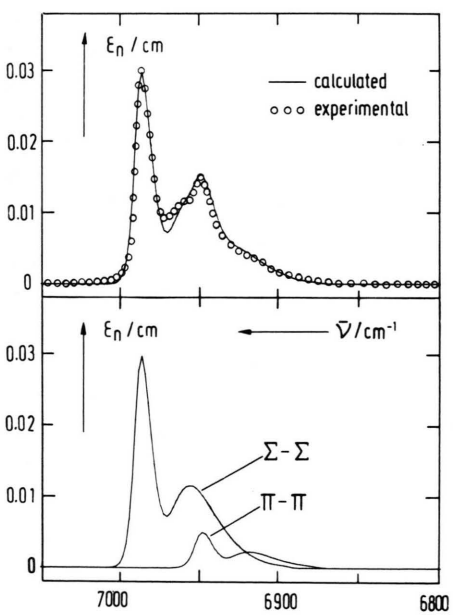

Fig. 4. Bandshape analysis of the stretching second overtone $3\nu_3$ absorption of pure CO_2 at 400 K and 0.1 $g \cdot cm^{-3}$ density. *Upper part:* Comparison of experimental and calculated bandshape. *Lower part:* Σ-Σ and Π-Π bandshapes (see text).

The variation of the band maximum position, $\bar{\nu}(\max)$, which is illustrated for the 6220 cm^{-1} mode in Fig. 5, follows the pattern outlined in Part I [2]: Temperature and density dependent P- and R-branch maxima occur at low and moderate compression. At intermediate CO_2 densities between 0.7 $g \cdot cm^{-3}$ and 1.0 $g \cdot cm^{-3}$, $\bar{\nu}(\max)$ is independent of temperature and decreases with density along a straight line constructed from $\bar{\nu}^g$, the gaseous pure vibrational transition, through $\bar{\nu}_m$, the arithmetic mean of the P- and R-branch positions. Toward the highest densities, the red-shift becomes weaker and, between 1.2 $g \cdot cm^{-3}$ and 1.4 $g \cdot cm^{-3}$, $\bar{\nu}(\max)$ is found to be independent of both, temperature and density.

Whereas the 6220 m^{-1} component may be influenced by Fermi resonance within the $3\nu_1 + \nu_3$, $2\nu_1 + 2\nu_2^0 + \nu_3$, $\nu_1 + 4\nu_2^0 + \nu_3$, $6\nu_2^0 + \nu_3$ tetrad, the $3\nu_3$ overtone (Fig. 6) should exhibit the T and ϱ dependence of a non Fermi resonating stretching mode. A contribution of the hot-band $3\nu_3$ transition on $\bar{\nu}(\max)$ only occurs at low densities where it makes the determination of $\bar{\nu}_m$ somewhat arbitrary. The essential features of the $\bar{\nu}(\max)$ vs. ϱ plots in Figs. 5 and 6 are similar. At intermediate densities, the $\bar{\nu}(\max)$ values linearly decrease with density without any pronounced temperature dependence. Toward higher densities also the variation with density disappears. At the highest density there seems to be a weak indication of $\bar{\nu}(\max)$ turning to higher wavenumbers, again. Blue-shifts of that kind are well-known from high-pressure studies on some vibrations in solid CO_2 [13]. They are interpreted as being due to strong repulsive interactions [14, 15].

Quantitative analysis of fluids via NIR spectroscopy is favoured by vibrational intensities being independent of density and temperature or showing only minor variations within an extended region of states. If B turns out to have a single value, the concentrations c of a species (at precisely known optical path length l) are directly obtained from the integrated absorbance of a characteristic mode, $\int A(\bar{\nu}) \cdot d\bar{\nu}$, which is an experimental quantity:

$$c = \int A(\bar{\nu})\, d\bar{\nu}/(B\, l)\,. \qquad (6)$$

Because of density tuning of Fermi resonance, as has been shown for the $\nu_1 + \nu_3$, $2\nu_2^0 + \nu_3$ Fermi diad [2], the absorption intensity is shifted between resonating modes. To overcome this problem, vibrational intensities are determined as an integral over the Fermi coupled species. For the $3\nu_1 + \nu_3$,

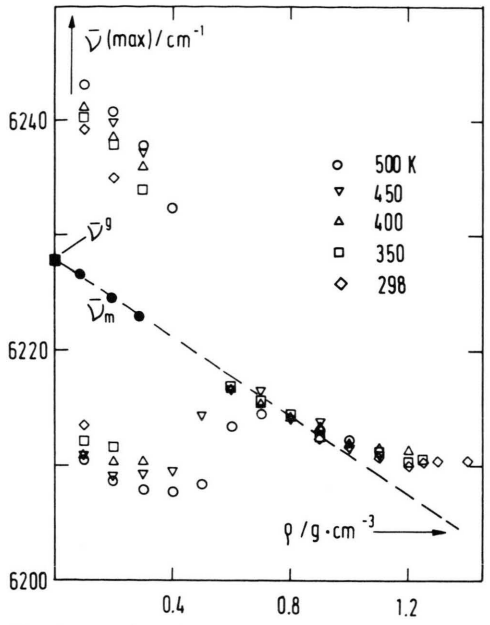

Fig. 5. Density dependence of band maximum position, $\tilde{\nu}$(max), of the 6220 cm^{-1} mode (with $\tilde{\nu}^g = 6227.9$ cm^{-1}) in pure CO_2 at temperatures between 298 K and 500 K ($\tilde{\nu}_m$ is the arithmetic mean of corresponding P- and R-branch maxima).

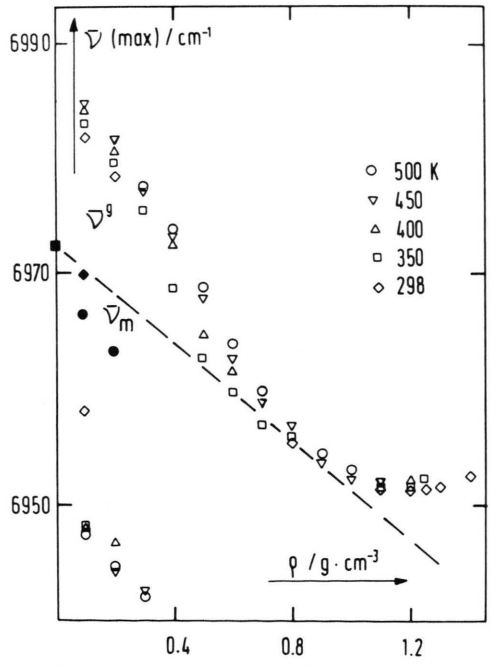

Fig. 6. Density dependence of band maximum position, $\tilde{\nu}$(max), of the $3\nu_3$ mode (with $\tilde{\nu}^g = 6972.6$ cm^{-1}) in pure CO_2 at temperatures between 298 K and 500 K ($\tilde{\nu}_m$ is the arithmetic mean of P- and R-branch maxima).

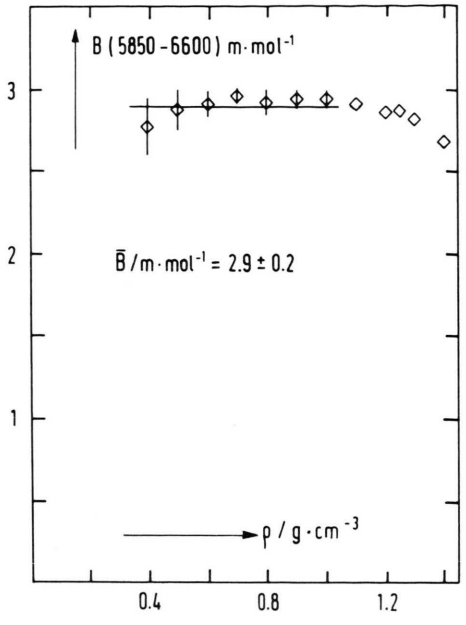

Fig. 7. Density dependence of the integrated molar absorptivity B of pure CO_2 in the wavenumber range from 5850 cm^{-1} to 6600 cm^{-1}. (Data points are mean values for the temperature range 298 K to 500 K.)

$2\nu_1 + 2\nu_2^0 + \nu_3$, $\nu_1 + 4\nu_2^0 + \nu_3$, $6\nu_2^0 + \nu_3$ tetrad thus integration is performed between 5850 cm^{-1} and 6600 cm^{-1} (Figure 7). At low absorbances, the large wavenumber range may give rise to an appreciable uncertainty due to an imperfect knowledge of the baseline for integration. For this reason, B values at CO_2 densities below 0.4 g · cm^{-3} are omitted in Figure 7. Toward the highest densities, B weakly decreases. In the extended density range from 0.4 g · cm^{-3} to 1.25 g · cm^{-3}, however, the vibrational intensity may be represented by a single value being independent of density and temperature within the limits of experimental accuracy:

$$B\,(5850-6600) = 2.9 \pm 0.2\ \text{m} \cdot \text{mol}^{-1}\,.$$

This value is in good agreement with gas phase vibrational intensities deduced from literature: 2.75 m · mol^{-1} [16] and 2.85 m · mol^{-1} [5].

The $3\nu_3$ second overtone vibrational intensity is determined from the wavenumber region 6700 cm^{-1} to 7300 cm^{-1} (Figure 8). Up to 1.0 g · cm^{-3}, the intensity is observed to be independent of temperature and density:

$$B\,(6700-7300) = 4.5 \pm 0.3\ \text{m} \cdot \text{mol}^{-1}\,,$$

which is slightly above the literature data for the gaseous state ($4.29\ m \cdot mol^{-1}$ [16], $4.32\ m \cdot mol^{-1}$ [17]). As the hot-band contribution to the integrated intensity strongly varies with temperature (Fig. 4), this result demonstrates that the molar absorptivities of $3\nu_3$ transitions from the ground state and from the first excited level of ν_2 should be similar. Toward higher densities, B slightly decreases. This behaviour, together with $\bar{\nu}(\max)$ being blue-shifted relative to the dashed line in Fig. 6, indicates the importance of repulsive interactions in highly compressed fluid CO_2.

Vibrational intensities obtained as a sum over Fermi coupled species, e.g. for the $\nu_1 + \nu_3$, $2\nu_2^0 + \nu_3$ diad [2], the $2\nu_1 + \nu_3$, $\nu_1 + 2\nu_2^0 + \nu_3$, $4\nu_2^0 + \nu_3$ triad [2], and the $3\nu_1 + \nu_3$, $2\nu_1 + 2\nu_2^0 + \nu_3$, $\nu_1 + 4\nu_2^0 + \nu_3$, $6\nu_2^0 + \nu_3$ tetrad (Fig. 7) within an extended temperature-density regime behave in a similar way as does B (6700 − 7300), the pure $3\nu_3$ second overtone intensity (Fig. 8). Assuming the vibrational intensities of the Fermi diad and tetrad, which have not been studied over the full density range, to be temperature independent and to remain constant throughout the density range up to $1.0\ g \cdot cm^{-3}$, as are the triad [2] and $3\nu_3$ intensities, quantitative NIR spectroscopy can be used up to 367 bar at 298 K and up to 2200 bar at 500 K. One important advantage of having several modes to probe CO_2 densities at high pressures and temperatures consists in the large difference in absorption intensity which enables quantitative work in a wide range of optical path lengths l or, at constant l, allows precise detection of CO_2 concentrations varying by orders of magnitude within one kinetic or thermodynamic experiment. The situation is illustrated in Fig. 9, which shows the NIR absorption of pure CO_2 (400 K, 600 bar, $0.8\ g \cdot cm^{-3}$) between $3300\ cm^{-1}$ and $7300\ cm^{-1}$. The four absorption bands, with increasing wavenumber, are due to the $\nu_1 + \nu_3$, $2\nu_2^0 + \nu_3$ diad, to the $2\nu_1 + \nu_3$, $\nu_1 + 2\nu_2^0 + \nu_3$, $4\nu_2^0 + \nu_3$ triad, to the $3\nu_1 + \nu_3$, $2\nu_1 + 2\nu_2^0 + \nu_3$, $\nu_1 + 4\nu_2^0 + \nu_3$, $6\nu_2^0 + \nu_3$ tetrad, and to $3\nu_3$. The logarithmic ε-scale demonstrates the strong variation of molar absorptivity by several orders of magnitude. If CO_2 concentrations are to be determined via NIR spectroscopy at absorbances in the band maxima not exceeding $A(\max) = 1$ (which ensures good quality of the spectra), from the $\varepsilon(\max)$ values of individual bands (Fig. 9) by means of (2), maximum optical pathlengths (for $A(\max) = 1$) are easily obtained: Values of $l(\max)$,

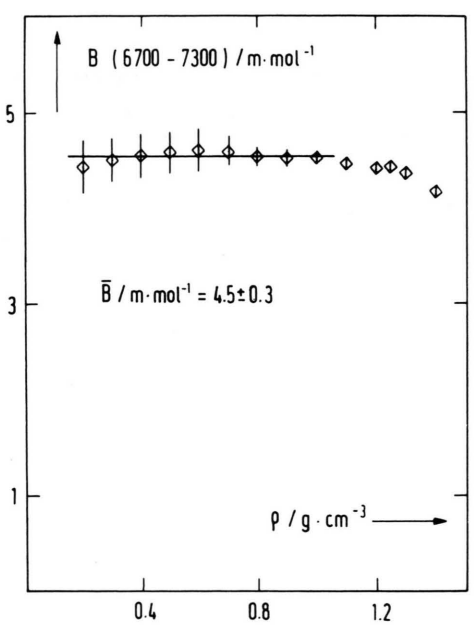

Fig. 8. Density dependence of the integrated molar absorptivity B of pure CO_2 in the wavenumber range from $6700\ cm^{-1}$ to $7300\ cm^{-1}$. (Data points are mean values for the temperature range 298 K to 500 K.)

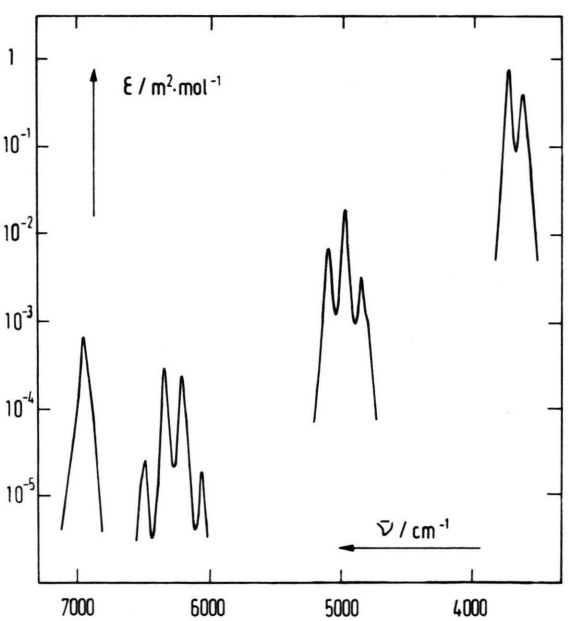

Fig. 9. Molar absorptivity ε of pure CO_2 at 400 K and 600 bar ($\varrho = 0.8\ g \cdot cm^{-3}$) in the near infrared region from $3300\ cm^{-1}$ to $7300\ cm^{-1}$.

e.g. for 0.8 g · cm^{-3} CO_2 density and 400 K, are calculated to be 0.072 mm, 2.6 mm, 173 mm, and 75 mm if analysis is performed via diad, triad, tetrad or $3\nu_3$ absorption, respectively. An alternative way of taking advantage of the large differences in ε(max) consists in performing experiments at constant pathlength where orders of magnitude changes in concentration can be measured with identical sensitivity by monitoring high concentrations at higher wavenumber, and vice versa (Fig. 9): If 0.8 g · cm^{-3} CO_2 at 400 K are measured (with A(max) = 1) at 75 mm pathlength via $3\nu_3$, the same maximum absorbance (at l = constant) is brought upon by 0.028 g · cm^{-3} and 0.00077 g · cm^{-3} in the triad and diad regions, respectively. With modern Fourier transform interferometers, the whole wavenumber range of Fig. 9, within about one second, can be precisely measured without any changes in optical configuration.

As, in addition, high performance is achieved in spectroscopic experiments with maximum absorbances slightly above and also well below unity, within one experiment (at identical pathlength) a concentration range covering at least four orders of magnitude can be studied via NIR. These attractive features have been illustrated for pure CO_2. It goes without saying that practical interest relates to mixtures where band overlap in many cases may pose problems. In the absence of specific intermolecular interactions, however, the knowledge of the pure component spectra, by using routine computer programs, will enable concentrations at high pressures and temperatures to be measured with good accuracy. The essential feature of NIR spectroscopy consists in the possibility of having, even in dense fluid systems, pathlengths of reasonable size, such as millimeters and centimeters, as compared to microns in the region of fundamental modes. The results obtained for CO_2 (e.g. Figs. 7–9) seem to be quite general and indicate promising applications of NIR spectroscopy for the quantitative study of a wide variety of fluid materials.

Acknowledgements

Financial support by the Deutsche Forschungsgemeinschaft (SFB 93) and by the Fonds der Chemischen Industrie is gratefully acknowledged. One of us, H. T., would like to thank the Max-Buchner-Forschungsstiftung for a fellowship.

[1] M. Buback, Z. Naturforsch. **39a,** 399 (1984).
[2] M. Buback, J. Schweer, and H. Tups, Z. Naturforsch. **41a,** 505 (1986).
[3] L. S. Rothman and L. D. G. Young, J. Quant. Spectrosc. Radiat. Transfer **25,** 505 (1981).
[4] C. P. Courtoy, Can. J. Phys. **35,** 608 (1957) and Ann. Soc. Sci. Bruxelles **73,** 5 (1959).
[5] R. A. Toth, R. H. Hunt, and E. K. Plyler, J. Mol. Spectrosc. **38,** 107 (1971).
[6] J. P. Maillard, M. Cuisenier, Ph. Arcas, E. Arie, and C. Amiot, Can. J. Phys. **58,** 1560 (1980).
[7] J. P. Bouanich, Nguyen-Van-Thanh, and H. Strapelias, J. Quant. Spectrosc. Radiat. Transfer **26,** 53 (1981).
[8] J. P. Bouanich, Nguyen-Van-Thanh, and I. Rossi, J. Quant. Spectrosc. Radiat. Transfer **30,** 9 (1983).
[9] M. Buback, J. Schweer, and H. Tups, Ber. Bunsenges. Phys. Chem. **89,** 545 (1985).
[10] C. B. Suarez and F. P. J. Valero, J. Mol. Spectrosc. **71,** 46 (1978).
[11] V. A. Boldyrev and K. P. Vasilevskii, Opt. Spectrosc. **35,** 476 (1973).
[12] G. Yamamoto, M. Tanaka, and T. Aoki, J. Quant. Spectrosc. Radiat. Transfer **9,** 371 (1969).
[13] R. C. Hanson and L. H. Jones, J. Chem. Phys. **75,** 1102 (1981).
[14] A. M. Benson and H. G. Drickamer, J. Chem. Phys. **27,** 1164 (1957).
[15] R. R. Wiederkehr and H. G. Drickamer, J. Chem. Phys. **28,** 311 (1958).
[16] L. S. Rothman and W. S. Benedict, Appl. Opt. **17,** 2605 (1978).
[17] T. G. Adiks, Opt. Spectrosc. **40,** 547 (1976).